Polímeros
ISSN 1678-5169 (Online)

https://doi.org/10.1590/0104-1428.20240025

ORIGINAL ARTICLES

Properties of regenerated cellulose films with silver nanoparticles and plasticizers[a]

Lays Furtado de Medeiros Souza Kataoka[1]*, Maria del Pilar Hidalgo Falla[2] and Sandra Maria da Luz[1,2]

[1]Programa de Pós-graduação em Ciências Mecânicas, Departamento de Engenharia Mecânica, Universidade de Brasília – UnB, Brasília, DF, Brasil

[2]Programa de Pós-graduação em Integridade de Materiais da Engenharia, Faculdade do Gama, Universidade de Brasília – UnB, Brasília, DF, Brasil

**lays.furtado94@gmail.com*

[a]**This paper has been partially presented at the 17th Brazilian Polymer Congress, held in Joinville, SC, 29/Oct - 02/Nov/2023.**

Abstract

Nanocomposite films from cellulose jute fibers can be promising for application in electronic devices, mainly when silver nanoparticles (AgNPs) are added, which increases their conductivity. This work studied the transmittance, conductivity, and thermal stability of regenerated cellulose films (RCF) by adding AgNPs and plasticizers. Carboxymethylcellulose (CMC), sorbitol, and glycerol plasticizers were incorporated at 15 wt.% and 0.5 wt.% of AgNPs. The resulting materials were studied using Ultraviolet-visible and Fourier Transform Infrared Spectroscopy, electrical analysis using the Van der Pauw method, and thermogravimetry. As a result, an average size of 9 nm for AgNPs was verified. Incorporating AgNP in the films decreased the transmittance by a minimum of 34% compared to pure RCF and reduced thermal stability by at least 10 ºC. Nanocomposites containing plasticizers showed an improved conductivity after incorporating these components, from 10^{-2} to 10^{-1} (S/cm).

Keywords: *regenerated cellulose films, silver nanoparticles, transmittance, conductivity, thermal stability.*

How to cite: Kataoka, L. F. M. S., Falla, M. D. P. H., & Luz, S. M. (2024). Properties of regenerated cellulose films with silver nanoparticles and plasticizers. *Polímeros: Ciência e Tecnologia*, *34*(3), e20240028. https://doi.org/10.1590/0104-1428.20240025

1. Introduction

Cellulose can be applied in various forms, such as fibers, films, and composite materials, for several industrial uses[1]. Among these forms, conductive regenerated cellulose films are studied primarily for their applications in high-value electronic devices such as sensors, transistors, solar cells, supercapacitors, electromagnetic shielding, and other elements[2]. To obtain cellulose, plants composed of lignocellulose containing a significant proportion of cellulose have attracted interest due to their abundant, renewable, and naturally occurring polymers. Jute (*Corchorus capsularis*) is among the natural fibers that stand out as one of the greatest and cheapest sources of cellulose[3], with several applications worldwide, and it is only surpassed by cotton[4].

Regenerated cellulose films are obtained in such a way that the cellulose's fibrous and semi-crystalline structure must be broken down in a dissolution process and then undergo a subsequent coagulation step[2]. Systems that use alkaline solutions such as sodium hydroxide (NaOH) for cellulose dissolution are considered more cost-effective, and toxic substances are not used or produced throughout the process. As a result, water becomes a potential coagulant in the NaOH aqueous dissolution system because it is easily accessible and presents controlled results, such as porosity[5].

Conductive materials such as metals, inorganic oxides, conductive polymers, and carbon materials can be physically or chemically introduced into their structure[2]. Among these, metal nanoparticles can be applied in polymeric films due to their potential to enhance the overall properties of polymeric materials, such as conductivity[6-8]. These conductive films can be promising candidates for the manufacture of electronic components, as seen in previous works, where silver nanoparticles provided increased conductivity of regenerated cellulose films[9]. A homogeneous morphology was also observed, without agglomerates, which indicates an increase in the degree of molecular orientation of the films obtained by the regenerated process of the samples, probably due to the plasticizing effect of carboxymethylcellulose (CMC) used to stabilize the silver nanoparticle solution. This effect can improve the physical and chemical properties of the films and allows for more application options for these conductive films[9].

The appropriate selection of the plasticizer is influenced by several factors, such as the compatibility between the polymers used and the desired final properties[10]. Plasticizers are components that occupy intermediate positions between long polymeric chains, effectively increasing the distance between them and reducing secondary intermolecular

interactions, making them suitable for applications requiring flexibility and ductility, such as sheets or thin films[11-13]. Various properties, such as tensile strength, compression, toughness, dimensional and thermal stability, surface aspects, and optical properties, can be modified by incorporating plasticizers into regenerated cellulose films[12].

Plasticizers derived from renewable sources such as CMC, sorbitol, and glycerol are compatible with RCF films that can improve the mechanical flexibility of films and modify other physicochemical properties, such as thermal stability improvement[14]. CMC is a water-soluble derivative obtained through cellulose, sodium hydroxide, and monochloroacetic acid suspension reaction. It is widely recognized as an important source of cellulose used to enhance the properties of biofilms[15]. Sorbitol is a polyol commonly used in producing films using polysaccharides as raw materials[16]. Glycerol is one of the most common plasticizers used, mainly in biodegradable films[17]. When used as a plasticizer, glycerol interacts with cellulose chains, increasing molecular mobility and, consequently, the hydrophilicity and flexibility of the plasticized films[18]. These regenerated cellulose conductive films can be seen as a more sustainable option than petrochemical polymers, given the use of renewable raw materials in their manufacture and their biodegradable characteristics.

In regenerated cellulose conductive films, the insertion of plasticizers such as CMC, sorbitol, and glycerol is still understudied. Various works on the insertion of plasticizers in regenerated cellulose films are found in the literature, but these do not involve films with the insertion of conductors. Therefore, there is a study gap in the literature. In addition to conductivity, factors such as transmittance, chemical composition, and application temperature range should be studied. Then, in this work, regenerated cellulose films with the incorporation of silver nanoparticles (AgNsP) and plasticizers were evaluated for transmittance, conductivity, and thermal stability.

2. Materials and Methods

2.1 Materials

The bleached jute cellulose was obtained in previous work[9]. The following chemicals of reagent grade were used: sodium borohydrate ($NaBH_4$, 98%, Dynamic), silver nitrate ($AgNO_3$, 99.9%, Neon), sodium carboxymethyl cellulose (CMC, Sigma–Aldrich), sodium hydroxide (NaOH, 97%, Greentec), sorbitol (98%, Dynamic), and glycerol (98%, Synth).

2.2 Synthesis and characterization of silver nanoparticles

To obtain the nanoparticle solution, 450 mL of an 18.0 x 10^{-6} mol/L $NaBH_4$ solution was kept below 3 °C in an ice bath and added to an Erlenmeyer flask under vigorous magnetic stirring. Through a burette, 150 mL of a 9.0 x 10^{-6} mol/L solution of $AgNO_3$ was added at an additional rate of 1 drop/s. The chemical reaction between $NaBH_4$ and $AgNO_3$ in those concentrations resulted in AgNPs at 250 ppm. To avoid silver nanoparticle aggregation, the solution was stabilized with 0.6 g of CMC, which has the function of coating the nanoparticles. The silver nanoparticle solution, prepared by drying a small drop on a copper grid, was characterized by Transmission Electronic Microscopy (TEM) in the JEOL JEM 1011 equipment, with a voltage of 40 kV. The ImageJ software took size measurements and statistical analysis of silver nanoparticle dimensions from TEM images.

2.3 Obtaining regenerated cellulose films with silver nanoparticles

The bleached jute cellulose was ground in an automatic analytical mill Quimis Q298A for 30 seconds. Depending on the sample, as shown in Table 1, each solution was prepared as follows: To obtain the RCF film, 2.2 g of cellulose was dissolved in 100 mL of a pre-cooled solution (-12°C for 18 h) containing 8% (w/v) NaOH solution. The solution was kept in a freezer for at least 18 h to reach around -12°C equilibrium to achieve the cooling conditions. Also, to obtain the RCF with the AgNPs, 26 mL of nanoparticle solution at 250 ppm was added to achieve 0.5 wt.% of silver nanoparticle content before the pre-cooling. To prepare the RCF films with the plasticizers, the CMC, sorbitol, and glycerol, in amounts corresponding to 15 wt.% for cellulose, were added to the pure RCF solution. The same process was performed for the nanocomposites, which resulted in nanocomposites containing 15 wt.% of plasticizer and 0.5 wt.% of silver nanoparticle. To dissolve the solution, all samples were submitted under vigorous stirring at 3000 rpm and room temperature every 7 min.

To mold the films and regenerate the cellulose, the mixture containing cellulose, and nanoparticles was subjected to centrifugation at 4000 rpm for 10 min to exclude the undissolved part and perform degassing. Then, 7 mL of the resulting solution was poured onto a polypropylene Petri dish with a diameter of 85 mm. The RCF and nanocomposite films were pre-dried at room temperature for 18 h until gelation. Afterward, the sample was immersed in a water bath (distilled water) at room temperature for 15 min to coagulate and regenerate the cellulose. Finally, the films were dried at room temperature for 48 h before the characterization.

2.4 Ultraviolet-visible spectroscopy (UV–Vis)

The RCF and nanocomposite films were assessed with Evolution 220 Thermo Scientific equipment to determine their transmittance. The films' transmittance spectra were analyzed across 200 to 800 nm wavelengths.

Table 1. Composition of regenerated cellulose films.

Sample	Plasticizer (wt.%)	AgNP (wt.%)
RCF	-	-
RCF - AgNP	-	0.5%
RCF - CMC	15% CMC	-
RCF - CMC - AgNP	15% CMC	0.5%
RCF - Sorbitol	15% Sorbitol	-
RCF - Sorbitol - AgNP	15% Sorbitol	0.5%
RCF - Glycerol	15% Glycerol	-
RCF - Glycerol - AgNP	15% Glycerol	0.5%

2.5 Fourier Transform Infrared (FTIR) spectroscopy

FTIR spectra of RCF and nanocomposite films were obtained using a Fourier-transform infrared spectrometer (NICOLET IS10, Thermo Scientific) by transmittance accessory from 500 to 4000 cm^{-1} with 64 scans collected at an interval of 4 cm^{-1}.

2.6 Electrical measurements of films by the Van der Pauw method

Using the Van der Pauw method to characterize thin films, the sheet resistance measurements of nanocomposite films were obtained through four-point measurements using the Agilent B1500A Semiconductor Device Analyzer. The samples were subjected to a current range from 100 uA to 1 mA with a 10 uA interval, up to a limit of 1 V. To calculate resistivity and conductivity, film thicknesses were measured with a Mitutoyo digital micrometer (error of 0.001mm), taken at 10 points across the material.

From the sheet resistance measurements (R_s), expressed in units of ohms per square ($\Omega/\square$) e and the uniform thickness of the films (t), the sheet resistivity (ρ_s) can be obtained using Equation 1.

$$\rho_s = R_s.t \quad [\Omega.cm] \tag{1}$$

Where the sheet conductivity (σ_s) can then be calculated using Equation 2:

$$\sigma_s = \frac{1}{\rho_s} \quad [S/cm] \tag{2}$$

2.7 Thermogravimetric Analysis (TGA)

The RCF and nanocomposite films were characterized via thermogravimetry analysis (TGA: SDT Q600 TA Instruments). Approximately 10 mg of each sample was analyzed in alumina pans. The analysis was conducted under a nitrogen atmosphere (flow rate 50 mL/min) and a heating rate of 10 °C min^{-1} from 30 to 600 °C.

3. Results and Discussion

3.1 Morphological characterization of silver nanoparticles (AgNP) and transmittance characterization of films

Figure 1 shows the transmission micrographs of the AgNP solution. The micrographs show that the nanoparticles are homogeneous in size. The average size found for the nanoparticles was 9.0 ± 2.0 nm, with spherical characteristics within the range typically obtained in the literature using the synthesis method from silver nitrate and sodium borohydride solutions[19].

Figure 2 shows the appearance of each studied film, according to Table 1. The incorporation of AgNPs changed the color of the films, which caused the samples to darken due to the yellowish color of the nanoparticle solution. Visually, the RCF—CMC—AgNP and RCF—Glycerol—AgNP films are opaquer, similar to the RCF—Glycerol film. Subsequently, UV-Vis spectroscopy reveals the effect of incorporating plasticizers and AgNPs on the optical properties of these films.

The transmittance of conductive films is an important factor to be evaluated, as the mutually opposing properties of conductivity and transparency using metallic conductive materials in films are challenging. This challenge may restrict their application in electronic devices like optoelectronics, including solar cells and touch screens[20,21]. Additionally, incorporating plasticizers into regenerated cellulose films can increase or decrease the transmittance of these films[22]. Therefore, UV-Vis investigated the effect of plasticizer and AgNP incorporation on the transmittance of regenerated cellulose films. The UV-Vis results and the transmittance values for the films at 550 nm are presented in Figure 3. The transmittance curve for all RCF films was observed throughout the wavelength range between 200 and 800 nm[9]. Figure 3 reveals low transmittance of the RCF - CMC - AgNP, RCF – Glycerol, and RCF - Glycerol - AgNP films in the UV region, suggesting that these samples have anti-UV

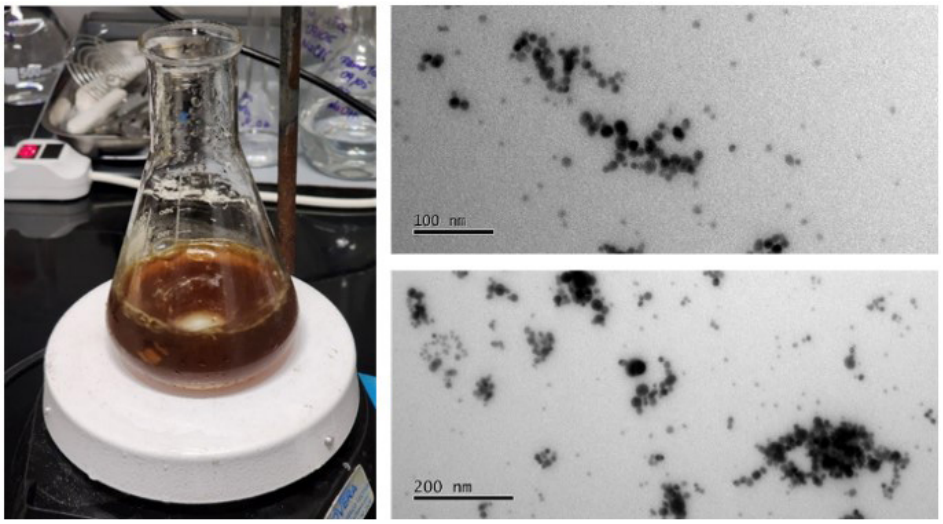

Figure 1. Transmission micrograph of the AgNP solution.

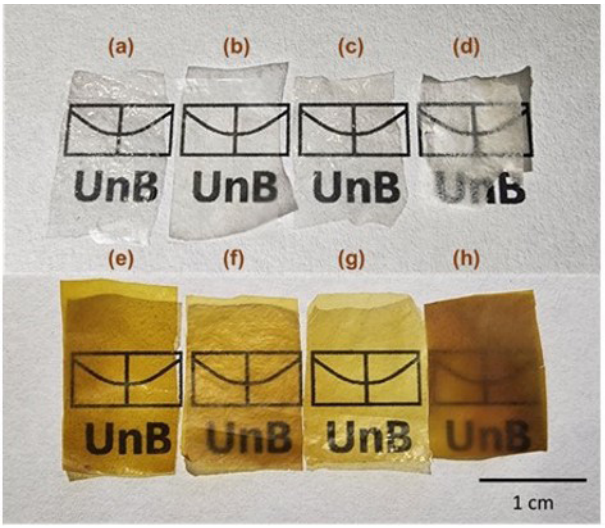

Figure 2. Appearance of RCF films and nanocomposites.

properties. In the visible region of the spectra, we noticed an increase in transmittance in all films. In addition, the transmittance of silver nanocomposites decreased with the incorporation of plasticizers since these components provide increased absorption, as seen in the literature[14].

The RCF sample obtained a high transmittance value, as reported in some studies with similar applications for regenerated cellulose films[2]. Incorporating sorbitol into RCF - Sorbitol increased the transmittance value to greater than pure RCF. However, containing plasticizers in RCF-CMC and RCF-Glycerol samples decreased the transmittance concerning RCF, with the latter experiencing a significant decrease upon adding glycerol.

The presence of a transmittance band, near 300-400 nm for the nanocomposite films containing AgNPs, indicates the existence of this component in the samples. The bands in this wavelength range are related to these spherical metal nanoparticles. As observed in the spectra, AgNPs with smaller sizes exhibit an absorption peak at shorter wavelengths[19]. Regarding the nanocomposite films, the RCF - Sorbitol - AgNP sample had lower transmittance than the RCF – AgNP. However, the plasticizer had the best result compared to the other plasticizers, in which the RCF - CMC - AgNP had the highest transmittance loss.

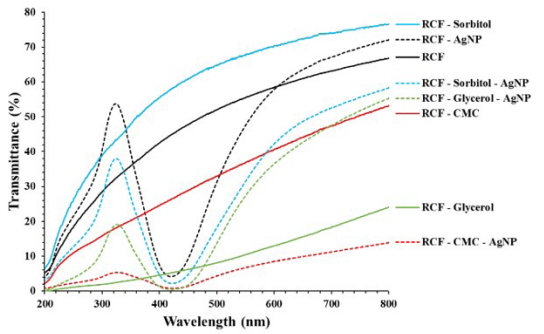

Sample	Transmittance at 550 nm (%)
RCF	54.4 ± 0.8
RCF - AgNP	9.3 ± 0.8
RCF - CMC	36.0 ± 0.8
RCF - CMC - AgNP	5.4 ± 1.0
RCF - Sorbitol	71.2 ± 2.4
RCF - Sorbitol - AgNP	31.2 ± 0.3
RCF - Glycerol	9.3 ± 0.8
RCF - Glycerol - AgNP	24.7 ± 2.4

Figure 3. UV-Vis spectra of RCF and nanocomposite films.

3.2 Characterization of films by Fourier Transform Infrared Spectroscopy (FTIR)

To identify the functional groups within the structure of the films and the chemical modifications resulting from the incorporation of plasticizers, the FTIR spectra of the controlled regenerated cellulose and nanocomposite films are shown in Figure 4. The absorption bands around 3440 cm^{-1} indicate the presence of cellulose due to the stretching of the hydrogen-bonded O-H, and around 2900 cm^{-1} corresponds to the stretching of the C-H functional group[14].

For nanocomposite films, a shift was observed in the C=O stretching from 1636 cm^{-1} to 1642 cm^{-1}, possibly due to the interaction between silver nanoparticles and the carbonyl group,

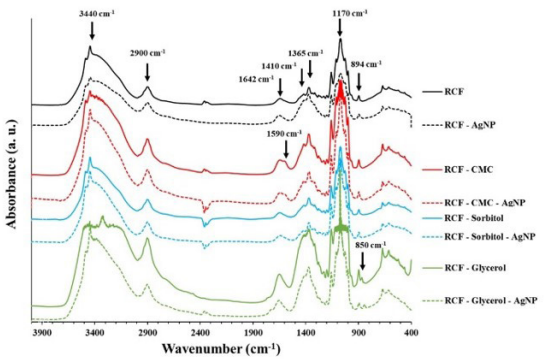

Figure 4. Fourier-transform infrared spectroscopy (FTIR) spectra for the same samples.

which suggests coordination between them[9,23]. The absorption band around 1410 cm^{-1} is associated with the symmetrical bending of CH_2 in cellulose, indicating correspondence with the cellulose II polymorph. A doublet at 1333-1311 cm^{-1} and a band at 1365 cm^{-1} were observed, corresponding to the angular bending of the COH and HCC bonds, ordinarily present in crystalline cellulose[24]. The peaks between 997 and 1200 cm^{-1} are also characteristic of cellulose. The peaks at 1170 cm^{-1}, 1040-1070 cm^{-1}, and 894 cm^{-1} are related to the stretching of the C-O vibrations and C-H deformation of the skeletal pyranose ring of cellulose[9]. At 997 cm^{-1}, there is a CO stretching peak. No chemical bond between cellulose and NaOH was identified from the FTIR [9].

Polyols, such as sorbitol and glycerol, exhibit bands ranging from 1500 to 1200 cm^{-1} attributed to the overlap of C-H in-plane and O-H bending in polyol molecules, coinciding with cellulose peaks[25]. Similarly, CMC also features characteristic peaks of cellulose, which it derives from. In films plasticized with CMC, the presence of an absorption band at 1590 cm^{-1} is observed, corresponding to the stretching vibration of carboxyl groups (COO-)[26,27], where the deprotonation of these groups is linked to the cellulose structure[28]. In glycerol-plasticized films, a peak around 850 cm^{-1} corresponds to the vibrations of the C-H groups[29].

The chemical changes in regenerated cellulose films can lead to physical alterations as the plasticizer connects to the biopolymer molecules, promoting greater mobility in the polymer chains and reducing the density between the molecules, affecting the film's optical properties. Therefore, investigating the transmittance of films is important to classify future applications of these films. The chemical changes in regenerated cellulose films can lead to physical changes as the plasticizer connects to the biopolymer molecules, which promotes greater mobility in the polymer chains and reduces the density between the molecules, affecting the film's optical properties. Therefore, investigating the transmittance of films is important to classify future applications of these films.

3.3 Electrical characterization of films

The concentration of AgNPs can affect the conductivity of regenerated cellulose films[9]. However, few studies have been conducted on the analysis of these films involving the incorporation of plasticizers. Therefore, given their two-dimensional nature, the Van der Pauw method allows the measurement of the electrical properties of these nanocomposite-regenerated cellulose films, reducing experimental errors such as those generated by contact misalignment[30]. Table 2 shows the conductivity values of the nanocomposite films.

Nanocomposites with plasticizers achieved a significant improvement in conductivity after incorporation of these components and ranged from 10^{-2} to 10^{-1} in relation to RCF - AgNP with the same nanoparticle content, with an increase of 292.3% for RCF - CMC - AgNP, 159.50% for RCF - Sorbitol - AgNP and 230.6% for RCF - Glycerol - AgNP.

The CMC plasticizer provided better conductivity values in the nanocomposite, followed by glycerol and sorbitol. The difference between the plasticized films RCF - CMC - AgNP with higher conductivity and RCF - Sorbitol - AgNP with lower conductivity was 51.2%. The difference between RCF - CMC - AgNP and RCF - Glycerol - AgNP was smaller at 18.7%.

Table 2. Conductivity data for nanocomposites.

Sample		Conductivity (S/cm)	Conductivity Average (S/cm) *1
RCF - AgNP	**1**	0.1014	0.06836 ±0.0230
	2	0.0536	
	3	0.0501	
RCF - CMC - AgNP	**1**	0.2898	0.2682 ± 0.0504
	2	0.1934	
	3	0.3087	
RCF - Sorbitol - AgNP	**1**	0.2060	0.1774 ± 0.0359
	2	0.1267	
	3	0.1994	
RCF - Glycerol - AgNP	**1**	0.2069	0.2260 ± 0.0506
	2	0.2953	
	3	0.1758	
RCF *2	[9]	3.28×10^{-2}	
RCF – 0.290% AgNP *2	[9]	5.32×10^{-2}	

*1 Three films of each nanocomposite studied were analyzed. For each film, electrical measurements were carried out in quadruplicate. *2 Literature data.

The electrical data for the pure RCF and the nanocomposite containing 0.290% AgNP described in Table 2, shows that increasing the content of silver nanoparticles from 0.290% to 0.5% in the RCF – AgNP (without plasticizer) provided an increase of 28.5% of conductivity. We also observed an increase of 717.8% in the conductivity of RCF - CMC – AgNP in relation to the conductivity of pure RCF[9].

Other works show the effect of increasing conductivity with plasticizer incorporation. Composite films of regenerated cellulose nanoparticles (RCNs) with poly(3,4—ethylenedioxythiophene) (PEDOT) achieved increased conductivity with the incorporation of RCNs that acted as a plasticizer, which improved the films' mechanical properties[31]. In blends of polyaniline and nitrile rubber, there was an increase in conductivity using the properties of imidazolium-based ionic liquids as plasticizers[32].

Conductive regenerated cellulose films in the order of magnitude of 10_{-2} to 10^{-1} S/cm, found for the nanocomposite films in this work, are promising for applications such as supercapacitors[33-35], strain sensors[36], electromagnetic interference shielding[37,38], anti-static cellulose films[39].

The AgNP are good electrical conductors but can also be good thermal conductors because they are metals. Therefore, it is important to study the thermal stability of films when incorporating this material and plasticizers.

3.4 Thermal Characterization (TG/DTG) of films

TG and DTG investigated the effect of incorporating plasticizers and AgNP on the thermal stability of regenerated cellulose films, and the curves are represented in Figure 5. Table 3 shows the thermal stability, peak temperatures of RCFs and nanocomposites, and weight loss from 100 °C to 600 °C.

Table 3. Thermal stability and degradation temperatures for plasticizers and regenerated films, with the addition of plasticizers and AgNP.

	Thermal Stability (°C)	$Peak_{Cellulose}$ (°C)	Weight Losses (%)				
			100 (°C)	200 (°C)	300 (°C)	400 (°C)	600 (°C)
RCF	230.3	334.1	12.2	13.7	31.0	74.7	80.4
RCF - AgNP	219.9	309.9	12.3	16.8	53.3	68.6	74.5
RCF - CMC	222.2	321.4	12.1	14.0	33.8	68.1	75.2
RCF - CMC - AgNP	197.2	303.4	11.3	14.7	50.0	71.0	77.6
RCF - Sorbitol	212.5	310.9	11.9	15.2	44.4	69.1	75.9
RCF - Sorbitol - AgNP	219.9	305.9	14.1	17.8	52.1	72.6	79.3
RCF - Glycerol	210.9	270.9	11.0	19.4	53.9	60.4	66.4
RCF - Glycerol - AgNP	201.0	252.9	11.6	17.6	52.4	57.7	62.3

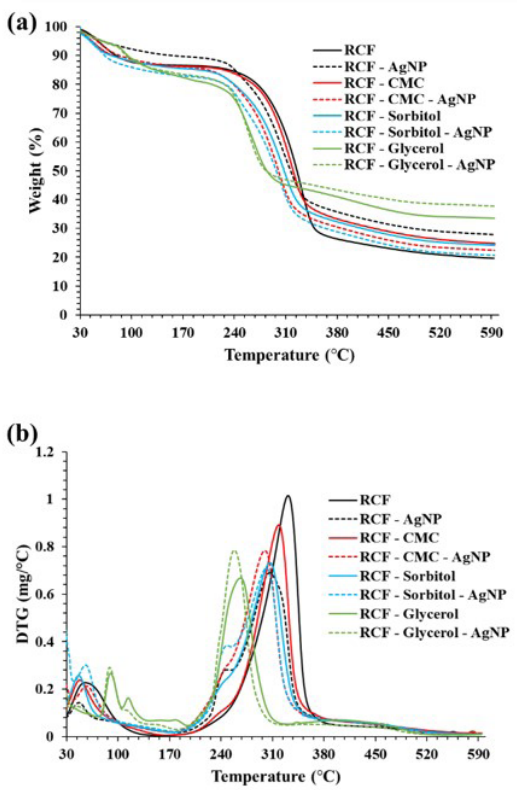

Figure 5. Curves (a) TGA, (b) DTG for RCF and nanocomposite films.

A thermal event occurs at temperatures below 100°C for all samples due to moisture loss[9]. We also include information regarding the thermal stability of the samples and the temperature of the main degradation peak corresponding to cellulose, which ranged from approximately 253°C to 334°C.

The least thermally stable samples where cellulose degradation peaks shifted to lower temperatures were those with glycerol, probably due to this component degrading at lower temperatures, as was previously observed in the literature[14], with a difference of 81.2 ºC from the RCF - Glycerol - AgNP for RCF. Therefore, the main degradation of these samples plasticized with glycerol occurred below 330 ºC and above 385 ºC for the others.

The thermal stability of all films with plasticizer incorporation was lower than pure RCF. The incorporation of plasticizer reduces the rigidity of the polymer chains. As a result, the thermal stability of the films was eventually reduced. Thus, incorporating plasticizer also reduced all films' initial and final decomposition temperature, possibly due to the mixing and interactions of the regenerated cellulose with the plasticizers[40].

Incorporating AgNP in all nanocomposite films shifted the cellulose degradation peak to lower temperatures. This can be correlated to the catalytic action of AgNPs on the cellulose polymer matrix, as they act as initiators and facilitators of thermal degradation of the polymer matrix due to their thermal conductivity, as seen in other works on polymer applications[41,42].

Optoelectronic applications are limited because the films studied in this work do not have high transmittance. However, the thermal stability together with the conductivity values in the order of magnitude of 10^{-2} to 10^{-1} S/cm, found for the nanocomposite films, are promising for applications such as supercapacitors[33-35], strain sensors[36], electromagnetic interference shielding[37,38], anti-static cellulose films[39], as seen in other papers.

4. Conclusions

Incorporating AgNPs and plasticizers into nanocomposite films decreased the transmittance compared to RCF films, making it difficult for light to pass through and limiting it to optical applications. AgNP nanocomposite films were less thermally stable than RCF without nanoparticles but did not impact large temperature differences. The FTIR spectra made it possible to visualize the film's functional groups, characteristics of cellulose, and plasticizers used. Furthermore, it also showed band shift, the possible interaction between AgNPs, and the carbonyl group in films. Nanocomposites containing plasticizers showed a significant improvement in conductivity after these components were incorporated, which ranged from 10^{-2} to 10^{-1} compared to RCF - AgNP for the same nanoparticle content. Therefore, incorporating plasticizers considerably improved the mobility of electrons in the cellulose polymer chain, making the material more conductive and potentially increasing application possibilities. The CMC plasticizer provided better conductivity values in the nanocomposite, followed by glycerol and sorbitol.

5. Author's Contribution

• **Conceptualization –** Lays Furtado de Medeiros Souza Kataoka; Sandra Maria da Luz.

• **Data curation –** Lays Furtado de Medeiros Souza Kataoka.

• **Formal analysis –** Lays Furtado de Medeiros Souza Kataoka; Maria del Pilar Hidalgo Falla.

• **Funding acquisition –** Sandra Maria da Luz.

• **Investigation –** Lays Furtado de Medeiros Souza Kataoka.

• **Methodology –** Lays Furtado de Medeiros Souza Kataoka.

• **Project administration –** Lays Furtado de Medeiros Souza Kataoka; Sandra Maria da Luz.

• **Resources –** Sandra Maria da Luz; Maria del Pilar Hidalgo Falla.

• **Software –** NA.

• **Supervision –** Sandra Maria da Luz; Maria del Pilar Hidalgo Falla.

• **Validation –** Lays Furtado de Medeiros Souza Kataoka; Sandra Maria da Luz.

• **Visualization –** Lays Furtado de Medeiros Souza Kataoka.

• **Writing – original draft –** Lays Furtado de Medeiros Souza Kataoka.

• **Writing – review & editing –** Lays Furtado de Medeiros Souza Kataoka; Sandra Maria da Luz.

6. Acknowledgements

The authors thank Fundação de Apoio à Pesquisa do Distrito Federal (FAPDF), Conselho Nacional de Desenvolvimento Científico e Tecnológico (CNPq), Fundação Coordenação de Aperfeiçoamento de Pessoal de Nível Superior (CAPES) and Universidade de Brasília (DPI, DPG, and BCE) for the financial support.

7. References

1. Abdul Khalil, H. P. S., Bhat, A. H., & Ireana Yusra, A. F. (2012). Green composites from sustainable cellulose nanofibrils: a review. *Carbohydrate Polymers*, *87*(2), 963-979. http://doi.org/10.1016/j.carbpol.2011.08.078.
2. Liu, X., Xiao, W., Ma, X., Huang, L., Ni, Y., Chen, L., Ouyang, X., & Li, J. (2020). Conductive regenerated cellulose film and its electronic devices – A review. *Carbohydrate Polymers*, *250*, 116969. http://doi.org/10.1016/j.carbpol.2020.116969. PMid:33049865.
3. Kataoka, L. F. M. S., Hidalgo Falla, M. D. P., & Luz, S. M. (2021). The influence of potassium hydroxide concentration and reaction time on the extraction cellulosic jute fibers. *Journal of Natural Fibers*, *19*(13), 6889-6901. http://doi.org/10.1080/15440478.2021.1934934.
4. Erdoğan, U. H., Seki, Y., Aydoğdu, G., Kutlu, B., & Akşit, A. (2016). Effect of different surface treatments on the properties of jute. *Journal of Natural Fibers*, *13*(2), 158-171. http://doi.org/10.1080/15440478.2014.1002149.
5. Budtova, T., & Navard, P. (2016). Cellulose in NaOH–water based solvents: a review. *Cellulose (London, England)*, *23*(1), 5-55. http://doi.org/10.1007/s10570-015-0779-8.
6. Meera, K., & Ramesan, M. T. (2023). Development of high-performance biopolymer nanocomposites derived from carboxymethyl chitosan/boehmite via green synthesis. *Polymer Composites*, *44*(3), 1135-1148. http://doi.org/10.1002/pc.27159.
7. Meera, K., Arun, K., & Ramesan, M. T. (2023). High performance biopolymer blend nanocomposites derived from cashew gum/polyvinyl alcohol/boehmite for flexible electronic devices. *Journal of Applied Polymer Science*, *140*(7), e54300. http://doi.org/10.1002/app.54300.
8. Ramesan, M. T., Subburaj, M., Mathew, G., & Bahuleyan, B. K. (2023). Utilization of copper sulphide nanoparticles for the development of cashew tree gum/chitin biopolymer blend nanocomposites. *Journal of Thermoplastic Composite Materials*, *36*(7), 984-1003. http://doi.org/10.1177/08927057211046282.
9. Kataoka, L. F. M. S., Leão, R. M., Gontijo, A. B., Falla, M. D. P. H., & Luz, S. M. (2022). Regenerated cellulose films from jute fibers applied in conductive nanocomposites. *Materials Today. Communications*, *33*, 104645. http://doi.org/10.1016/j.mtcomm.2022.104645.
10. Cheremisinoff, N. P. (1998). *Advanced polymer processing operations*. USA: Noyes Publications.
11. Vanin, F. M., Sobral, P. J. A., Menegalli, F. C., Carvalho, R. A., & Habitante, A. M. Q. B. (2005). Effects of plasticizers and their concentrations on thermal and functional properties of gelatin-based films. *Food Hydrocolloids*, *19*(5), 899-907. http://doi.org/10.1016/j.foodhyd.2004.12.003.
12. Callister, W. D., Jr. (2007). *Materials science and engineering: an introduction*. USA: John Wiley & Sons.
13. Meera, K., & Ramesan, M. T. (2023). Tailoring the performance of boehmite nanoparticles reinforced carboxymethyl chitosan/cashew gum blend nanocomposites via green synthesis. *Polymer*, *268*, 125706. http://doi.org/10.1016/j.polymer.2023.125706.
14. Pang, J., Liu, X., Zhang, X., Wu, Y., & Sun, R. (2013). Fabrication of cellulose film with enhanced mechanical properties in ionic liquid 1-allyl-3-methylimidazolium chloride (AmimCl). *Materials (Basel)*, *6*(4), 1270-1284. http://doi.org/10.3390/ma6041270. PMid:28809209.
15. Caraschi, J. C., & Campana, S. P., Fo. (1999). Influência do grau de substituição e da distribuição de substituintes sobre as propriedades de equilíbrio de carboximetilcelulose em solução aquosa. *Polímeros: Ciência e Tecnologia*, *9*(2), 70-77. http://doi.org/10.1590/S0104-14281999000200015.
16. McHugh, T. H., & Krochta, J. M. (1994). Sorbitol- vs glycerol-plasticized whey protein edible films: integrated oxygen permeability and tensile property evaluation. *Journal of Agricultural and Food Chemistry*, *42*(4), 841-846. http://doi.org/10.1021/jf00040a001.
17. Pérez, O. E., Sánchez, C. C., Pilosof, A. M. R., & Patino, J. M. R. (2008). Dynamics of adsorption of hydroxypropyl methylcellulose at the air-water interface. *Food Hydrocolloids*, *22*(3), 387-402. http://doi.org/10.1016/j.foodhyd.2006.12.005.
18. Mali, S., Sakanaka, L. S., Yamashita, F., & Grossmann, M. V. E. (2005). Water sorption and mechanical properties of cassava starch films and their relation to plasticizing effect. *Carbohydrate Polymers*, *60*(3), 283-289. http://doi.org/10.1016/j.carbpol.2005.01.003.
19. Leopold, N., & Lendl, B. (2003). A new method for fast preparation of highly surface-enhanced Raman scattering (SERS) active silver colloids at room temperature by reduction of silver nitrate with hydroxylamine hydrochloride. *The Journal of Physical Chemistry B*, *107*(24), 5723-5727. http://doi.org/10.1021/jp027460u.

20. Wassei, J. K., & Kaner, R. B. (2010). Graphene, a promising transparent conductor. *Materials Today*, *13*(3), 52-59. http://doi.org/10.1016/S1369-7021(10)70034-1.
21. Ma, X., Deng, Q., Wang, L., Zheng, X., Wang, S., Wang, Q., Chen, L., Huang, L., Ouyang, X., & Cao, S. (2019). Cellulose transparent conductive film and its feasible use in perovskite solar cells. *RSC Advances*, *9*(17), 9348-9353. http://doi.org/10.1039/C9RA01301F. PMid:35520713.
22. Kaco, H., Zakaria, S., Chia, C. H., & Zhang, L. (2014). Transparent and printable regenerated kenaf cellulose/PVA film. *BioResources*, *9*(2), 2167-2178. http://doi.org/10.15376/biores.9.2.2167-2178.
23. Yang, Q., Wang, F., Tang, K., Wang, C., Chen, Z., & Qian, Y. (2003). The formation of fractal Ag nanocrystallites via γ-irradiation route in isopropyl alcohol. *Materials Chemistry and Physics*, *78*(2), 495-500. http://doi.org/10.1016/S0254-0584(02)00379-6.
24. Ludueña, L. N., Vecchio, A., Stefani, P. M., & Alvarez, V. A. (2013). Extraction of cellulose nanowhiskers from natural fibers and agricultural byproducts. *Fibers and Polymers*, *14*(7), 1118-1127. http://doi.org/10.1007/s12221-013-1118-z.
25. Pourfarzad, A., Ahmadian, Z., & Habibi-Najafi, M. B. (2018). Interactions between polyols and wheat biopolymers in a bread model system fortified with inulin: a Fourier transform infrared study. *Heliyon*, *4*(12), e01017. http://doi.org/10.1016/j.heliyon.2018.e01017. PMid:30560212.
26. Su, J.-F., Huang, Z., Yuan, X.-Y., Wang, X.-Y., & Li, M. (2010). Structure and properties of carboxymethyl cellulose/soy protein isolate blend edible films crosslinked by Maillard reactions. *Carbohydrate Polymers*, *79*(1), 145-153. http://doi.org/10.1016/j.carbpol.2009.07.035.
27. Mondal, M. I. H., Yeasmin, M. S., & Rahman, M. S. (2015). Preparation of food grade carboxymethyl cellulose from corn husk agrowaste. *International Journal of Biological Macromolecules*, *79*, 144-150. http://doi.org/10.1016/j.ijbiomac.2015.04.061. PMid:25936282.
28. Tavares, K. M., Campos, A., Luchesi, B. R., Resende, A. A., Oliveira, J. E., & Marconcini, J. M. (2020). Effect of carboxymethyl cellulose concentration on mechanical and water vapor barrier properties of corn starch films. *Carbohydrate Polymers*, *246*, 116521. http://doi.org/10.1016/j.carbpol.2020.116521. PMid:32747230.
29. Ayala, G., Agudelo, A. C., & Vargas, R. (2012). Effect of glycerol on the electrical properties and phase behavior of cassava starch biopolymers. *Dyna*, *79*(171), 138-147. Retrieved in 2024, March 24, from http://www.scielo.org.co/pdf/dyna/v79n171/a18v79n171.pdf
30. Van Der Pauw, L. J. (1958). A method of measuring specific resistivity and Hall effect of discs of arbitrary shapes. *Philips Research Reports*, *13*(1), 1-9.
31. Choi, S. M., Han, S. S., & Shin, E. J. (2020). Highly stretchable conductive nanocomposite films using regenerated cellulose nanoparticles. *ACS Applied Polymer Materials*, *2*(10), 4387-4398. http://doi.org/10.1021/acsapm.0c00294.
32. Prudêncio, L., Camilo, F. F., & Faez, R. (2014). Líquidos iônicos como plastificantes em blendas de borracha nitrílica/polianilina. *Quimica Nova*, *37*(4), 618-623. http://doi.org/10.5935/0100-4042.20140103.
33. Liu, S., Yu, T., Wu, Y., Li, W., & Li, B. (2014). Evolution of cellulose into flexible conductive green electronics: A smart strategy to fabricate sustainable electrodes for supercapacitors. *RSC Advances*, *4*(65), 34134-34143. http://doi.org/10.1039/C4RA07017H.
34. Zhao, D., Chen, C., Zhang, Q., Chen, W., Liu, S., Wang, Q., Liu, Y., Li, J., & Yu, H. (2017). High performance, flexible, solid-state supercapacitors based on a renewable and biodegradable mesoporous cellulose membrane. *Advanced Energy Materials*, *7*(20), 1700739. http://doi.org/10.1002/aenm.201700739.
35. Tian, J., Peng, D., Wu, X., Li, W., Deng, H., & Liu, S. (2017). Electrodeposition of Ag nanoparticles on conductive polyaniline/cellulose aerogels with increased synergistic effect for energy storage. *Carbohydrate Polymers*, *156*, 19-25. http://doi.org/10.1016/j.carbpol.2016.09.005. PMid:27842813.
36. Mun, S., Zhai, L., Min, S.-K., Yun, Y., & Kim, J. (2016). Flexible and transparent strain sensor made with silver nanowire-coated cellulose. *Journal of Intelligent Material Systems and Structures*, *27*(8), 1011-1018. http://doi.org/10.1177/1045389X15577651.
37. Chen, J., Xu, J., Wang, K., Qian, X., & Sun, R. (2015). Highly thermostable, flexible, and conductive films prepared from cellulose, graphite, and polypyrrole nanoparticles. *ACS Applied Materials & Interfaces*, *7*(28), 15641-15648. http://doi.org/10.1021/acsami.5b04462. PMid:26135618.
38. Lee, T.-W., & Jeong, Y. G. (2015). Regenerated cellulose/multiwalled carbon nanotube composite films with efficient electric heating performance. *Carbohydrate Polymers*, *133*, 456-463. http://doi.org/10.1016/j.carbpol.2015.06.053. PMid:26344302.
39. Huang, H.-D., Liu, C.-Y., Zhang, L.-Q., Zhong, G.-J., & Li, Z.-M. (2015). Simultaneous reinforcement and toughening of carbon nanotube/cellulose conductive nanocomposite films by interfacial hydrogen bonding. *ACS Sustainable Chemistry & Engineering*, *3*(2), 317-324. http://doi.org/10.1021/sc500681v.
40. Khan, A., Niazi, M. B. K., Naqvi, S. R., & Farooq, W. (2018). Influence of plasticizers on mechanical and thermal properties of methyl cellulose-based edible films. *Journal of Polymers and the Environment*, *26*(1), 291-300. http://doi.org/10.1007/s10924-017-0953-1.
41. Silva, W. T. A. (2021). *Espumas de poliestireno impregnadas com nanopartículas de prata para a redução catalítica de p-nitrofenol em água* (Master's thesis). Universidade Estadual da Paraíba, Campina Grande.
42. Costa, F. S. (2016). *Desenvolvimento de nanocompósitos de poli(3-hidroxibutirato-co-3-hidroxivalerato) com nanopartículas de prata* (Master's thesis). Universidade Federal de São Paulo, São José dos Campos.

Received: Mar. 18, 2024
Revised: June 18, 2024
Accepted: June 24, 2024